

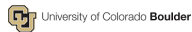
# ETG Turbulence Isotropization

Stefan Tirkas<sup>1</sup>Hoatian Chen<sup>1</sup>   Gabriele Merlo<sup>2</sup>   Scott Parker<sup>1</sup>

<sup>1</sup>CIPS, University of Colorado, Boulder

<sup>2</sup>University of Texas, Austin

November 2, 2020



# Outline

- 1 Drift Wave Instabilities
- 2 Hasegawa-Mima Fluid Model
- 3 Zonal Flow Excitation

# Drift Wave Instabilities

- Drift waves are characterized as density, temperature or pressure fluctuations in plasmas.
- Modes relevant to tokamak physics include ion-temperature-gradient modes (ITG), electron-temperature-gradient modes (ETG), and trapped electron modes (TEM).
- Low-frequency drift wave turbulence is largely responsible for the anomalous transport of plasma particles across magnetic field lines [1].



# Ion-Temperature-Gradient Mode Growth

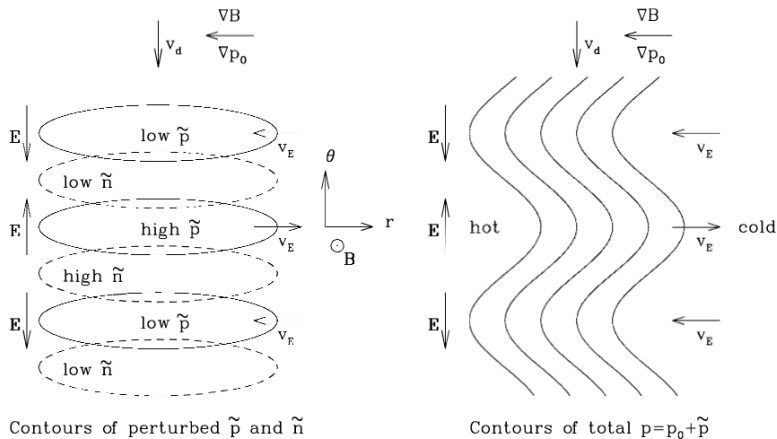
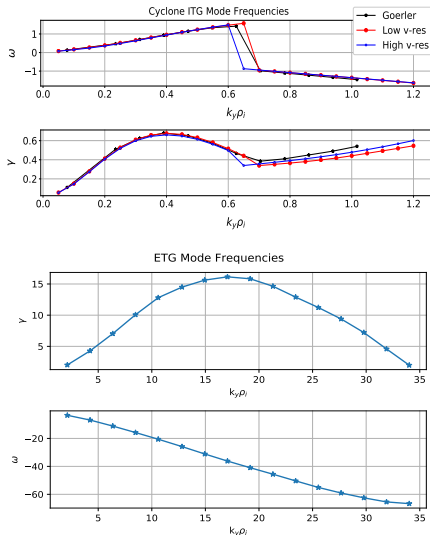


**Figure:** Simple picture of ITG instability [2].

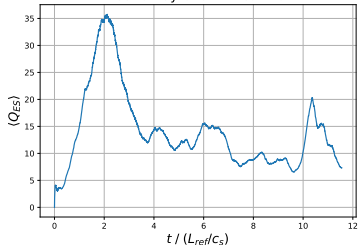
# ETG Simulation in GENE



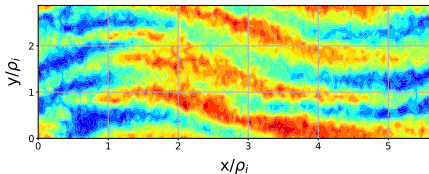
- Successful reproduction of Görler benchmark with kinetic ions and electrons [3].
- Conversion of ITG to ETG flux-tube case prior to running non-linear simulations.

# ETG "Streamers" in GENE

Electron GyroBohm Heat Flux



$\phi$



- ETG turbulence in toroidal gyrokinetic simulations is associated with radially elongated "streamers".
- Multiscale turbulence simulations have shown that streamers dominate electron heat flux and lead to experimental tokamak heat flux values [4].

# Hasegawa-Mima Fluid ETG Model

- Partial differential equation derived from fluid continuity and momentum equations.
- Approximations made that are useful to describing turbulence in tokamak plasmas.
  - Cyclotron motion periods much smaller than time scales that quantities of interest change on  $(B, \Phi, n)$ .
  - Long length scales along  $\hat{b}$ -direction -  $k_{\parallel}/k_{\perp} \equiv \epsilon \ll 1$ .
  - Quasi-neutrality of particle densities is enforced.
  - Adiabatic ions.
  - Isothermal equation of state, with  $\delta P_e = \delta n_e T_e$  ( $\delta T_e = 0$ ).
- Shown to cause isotropic behavior for long wavelength modes as well as an inverse energy-cascade [5].

# Hasegawa-Mima Equations

We start with the fluid continuity and momentum equations with  $\tau = T_e/T_i$ , where we have already taken the approximations discussed on the previous slide:

$$\frac{\partial n_e}{\partial t} + \nabla \cdot (n_e \vec{v}_e) = 0, \quad (1)$$

$$m_e \frac{d\vec{v}_e}{dt} = (1 + \tau) e \nabla \delta \Phi - \frac{e}{c} \vec{v}_e \times \vec{B} - \frac{\nabla P_e}{n_e}. \quad (2)$$

Then  $\vec{v}_e$  is solved for using (2) and plugged into (1), dropping terms higher order than  $\epsilon$  to get a final PDE describing the evolution of  $\delta \Phi$ . The derivation is carried out in Appendix A.



# Hasegawa-Mima Equations

Taking a standard electron dynamic normalization,

$$\begin{aligned}\Phi &= \frac{e\delta\Phi}{T_i}, \quad -\frac{1}{r_n} = \frac{\partial_x n_e}{n_e}, \quad -\frac{1}{r_t} = \frac{\partial_x T_e}{T_e}, \quad \eta_e = \frac{r_n}{r_t}, \\ \rho_e &= \sqrt{\frac{\tau m_e}{m_i}} \rho_i, \quad \vec{x} = \frac{\vec{X}}{\rho_e}, \quad t = \frac{\rho_e}{r_n} \omega_{ce} t,\end{aligned}\tag{3}$$

and plugging into (10) gives the form of the H-M ETG model,

$$\begin{aligned}-\left(1 - \frac{1+\tau}{2\tau} \nabla_{\perp}^2\right) \partial_t \Phi &+ \frac{1+\tau}{2\tau} \frac{r_n^2}{\rho_e^2} \partial_t^{-1} \nabla_{\parallel}^2 \Phi + \frac{(1+\tau)(1+\eta_e)}{4\tau} \partial_y \nabla_{\perp}^2 \Phi \\ &+ \frac{1+\eta_e}{2\tau} \partial_y \Phi + \frac{(1+\tau)^2}{\tau^2} \frac{r_n}{4\rho_e} (\hat{b} \times \nabla_{\perp} \Phi \cdot \nabla_{\perp}) \nabla_{\perp}^2 \Phi = 0.\end{aligned}\tag{4}$$

# Hasegawa-Mima Equations

We drop the higher order parallel gradient term and simplify the bracketed expression for a 2-D slab geometry to find the final form,

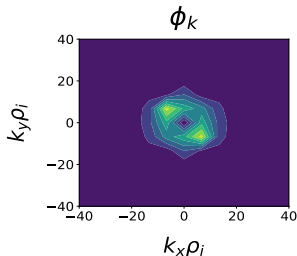
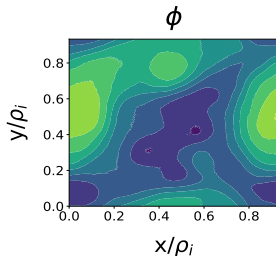
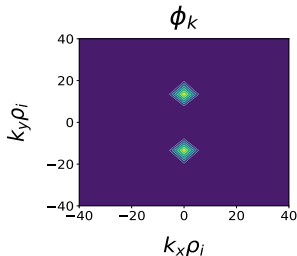
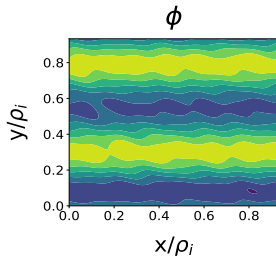
$$\begin{aligned}\partial_t\left[\Phi - \frac{1+\tau}{2\tau}\zeta\right] &= \frac{(1+\tau)(1+\eta_e)}{4\tau}\zeta_y + \frac{1+\eta_e}{2\tau}\Phi_y \\ &+ \frac{(1+\tau)^2}{\tau}\frac{r_n}{4\rho_e}[\Phi_x\zeta_y - \zeta_x\Phi_y],\end{aligned}\tag{5}$$

where  $\zeta = \nabla^2\Phi$  and  $x, y$  subscripts denote partial derivatives. The non-linear terms lead to rotation in  $k$ -space and eventually isotropization.

# Pseudo-Spectral Solver

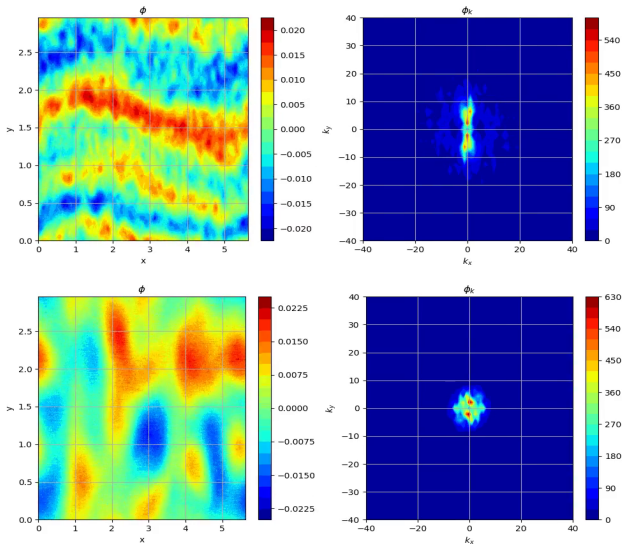
- Equation (6) is solved numerically using the pseudo-spectral method.
  - Fourier transform the equation and get  $\zeta = -(k_x^2 + k_y^2)\Phi$ .
  - Inverse Fourier transform  $\zeta_{x,y}$  and  $\Phi_{x,y}$  back into real space.
  - Calculate the non-linear products between  $\zeta$  and  $\Phi$  in real space and then Fourier transform the products so they can be added to the other terms in Fourier space.
  - Time advance  $\Phi$  discretely.
- Time advancement is done using the 4<sup>th</sup> order Runge-Kutta method.
- The pseudo-spectral method requires de-aliasing of modes due to non-linear terms. This is explored in Appendix B.

# ETG H-M Results



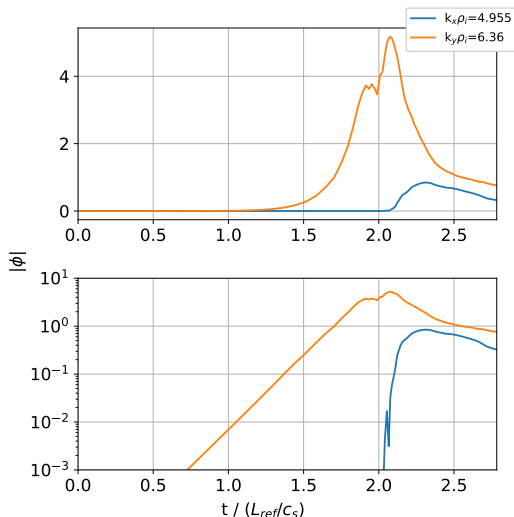
- Results of H-M code. Initial condition (above) isotropizes at late time (below).
- Parameters:
  - $\tau = 1$
  - $\eta_e = 3$
  - $r_n/\rho_i = 500$

# GENE ETG Streamer Test



- Test of GENE saturated ETG results into H-M code. Initial condition (above) isotropizes at late time (below).
- Inverse energy cascade observed as well.

# Zonal Flow Excitation



- Zonal flow can be spontaneously excited by intermediate-scale ETG turbulence in tokamak geometries -  $k_{\perp}\rho_e \ll 1 \ll k_{\perp}\rho_i$ .
- Plan to carry out large-scale ETG simulations with GENE to compare to theory of zonal flow excitation by ETG modes.

# Four-Wave Weak Turbulence Model

$$\begin{aligned}(\partial_t + \gamma_z(1 + d_z k_z^2 \rho_e^2))\chi_z A_z &= \sqrt{\pi/2} W k_z^3 \rho_e^3 (A_+ A_0^* a_n^* - A_-^* A_0 a_n), \\ [\partial_t + i\Delta - \gamma_s] A_+ &= -W k_z \rho_e A_z A_0 / \sqrt{2\pi}, \\ [\partial_t + i\Delta - \gamma_s] A_- &= W k_z \rho_e A_z^* A_0 / \sqrt{2\pi}, \\ [\partial_t - \gamma_n] A_0 &= -W k_z \rho_e (A_z A_- - A_z^* A_+ ) / \sqrt{2\pi}, \\ (\partial_t - 2\gamma_n) |A_0|^2 &= (2\gamma_s - \partial_t) (|A_+|^2 + |A_-|^2)\end{aligned}$$

- $A_z \equiv$  Zonal Flow Amp.
- $A_{\pm} \equiv$  Sideband Amp.'s
- $A_0 \equiv$  ETG Pump Wave
- $a_n \equiv$  Parallel coupling fn.
- $W \equiv$  Bandwidth
- $\gamma_{z,n,s} \equiv$  Growth rates
- $\chi_z \equiv$  Susceptibility
- $k_z \equiv$  radial k

## References

- W. Horton, Rev. Mod. Phys. **71**, 735 (1999).
- M. A. Beer, *Ph.D. Thesis - Gyrofluid Models of Turbulent Transport in Tokamaks*, Princeton University (1994).
- T. Görler *et al*, Phys. Plasmas **23**, 072503 (2016).
- N.T. Howard *et al* 2016 Nucl. Fusion **56** 014004
- A. Hasegawa and Y. Kodama, Phys. Rev. Lett. **41**, 1470 (1978).



# Appendix A: H-M Fluid Model

We break up (2) into parallel and perpendicular components by taking a dot product with  $\hat{b}$  to find,

$$\frac{d\vec{v}_{e,\parallel}}{dt} = (1 + \tau) \frac{e}{m_e} \partial_t^{-1} \nabla_{\parallel} \delta\Phi \Rightarrow v_{\parallel} \simeq (1 + \tau) \frac{k_{\parallel} e \delta\Phi}{m_e \omega}, \quad (6)$$

$$\frac{d\vec{v}_{e,\perp}}{dt} = (1 + \tau) \frac{e}{m_e} \nabla_{\perp} \delta\Phi - \omega_{c,e} \vec{v}_{e,\perp} - \frac{\hat{b} \times \nabla P_e}{m_e n_e}. \quad (7)$$

# Appendix A: H-M Fluid Model

Then we can split up  $\vec{v}_e$  by ordering

$$\begin{aligned}\vec{v}_{e,0} &= \vec{v}_{\parallel} + \vec{v}_{\perp,0} = \vec{v}_{\parallel} + (1 + \tau) \vec{v}_E + \vec{v}_D, \\ \vec{v}_{e,1} &= \vec{v}_{\perp,1} = -\frac{1}{\omega_{c,e}} (\partial_t + \vec{v}_{e,0} \cdot \nabla) (\hat{b} \times \vec{v}_{e,0}) \\ &\simeq \frac{e(1 + \tau)}{m_e \omega_{c,e}^2} \partial_t \nabla_{\perp} \delta \Phi - \left[ \frac{\vec{b} \times \nabla P_e}{n_e} \cdot \nabla_{\perp} \right] \frac{e(1 + \tau)}{m_e^2 \omega_{c,e}^3} \nabla_{\perp} \delta \Phi \\ &\quad + \frac{e^2(1 + \tau)^2}{m_e^2 \omega_{c,e}^3} [\hat{b} \times \nabla_{\perp} \delta \Phi \cdot \nabla_{\perp}] \nabla_{\perp} \delta \Phi.\end{aligned}\tag{8}$$

# Appendix A: H-M Fluid Model

Now, with incompressibility to lowest order,  $\nabla \cdot \vec{v}_{e,0,\perp} = 0$  and so (1) becomes,

$$\partial_t \delta n_e + n_e \nabla \cdot (\vec{v}_{\parallel} + \vec{v}_{e,1}) + \nabla \delta n_e \cdot \vec{v}_D + (1 + \tau) \delta n_e \cdot \vec{v}_E = 0, \quad (9)$$

and plugging in  $\delta n_e = \delta n_i$ , we find that to order  $\epsilon$ ,

$$\begin{aligned} & -n_e \partial_t \frac{e\delta\Phi}{T_i} + n_e(1 + \tau) \frac{e}{m_e} \partial_t^{-1} \nabla_{\parallel}^2 \delta\Phi + \frac{en_e(1 + \tau)}{m_e \omega_{c,e}^2} \partial_t \nabla_{\perp}^2 \delta\Phi \\ & - \frac{e(1 + \tau)}{m_e^2 \omega_{c,e}^3} [\hat{b} \times \nabla P_e \cdot \nabla_{\perp}] \nabla_{\perp}^2 \delta\Phi + \frac{e^2 n_e (1 + \tau)^2}{m_e^2 \omega_{c,e}^3} [\hat{b} \times \nabla_{\perp} \delta\Phi \cdot \nabla_{\perp}] \nabla_{\perp}^2 \delta\Phi \\ & + \nabla_{\perp} \frac{e\delta\Phi}{T_i} \cdot \frac{\hat{b} \times \nabla P_e}{m_e \omega_{c,e}} + \frac{e(1 + \tau)}{m_e \omega_{c,e}} \nabla n_e \cdot \hat{b} \times \nabla \Phi = 0. \end{aligned} \quad (10)$$

## Appendix B: Pseudo-Spectral De-Aliasing

